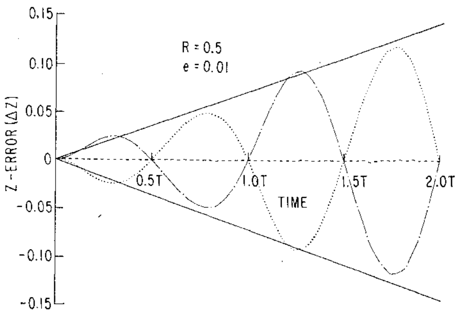

Fig. 3 Eccentricity error of the circular reference orbit solution in the three candidate coordinate systems: z axis.

matrix for an elliptic reference orbit to determine the effect of a small value of eccentricity on these terms. The secular terms are found to be linear in time and also linear in $\delta a/a$. In the local vertical coordinate system (LVCS) of this Note, the secular terms in position variation are

$$x = -1.5V_x t(\delta a)/a \tag{5}$$

$$z = -1.5V_z t(\delta a)/a \tag{6}$$

where

$$V_x = \mu(1 + e \cos f)/h \tag{7}$$

$$V_z = \mu e(\sin f)/h \tag{8}$$

In the local tangent coordinate system (LTCS) the corresponding terms are

$$x = -1.5Vt(\delta a)/a \tag{9}$$

$$z = 0 \tag{10}$$

where

$$V = \mu(1 + 2e \cos f + e^2)^{1/2}/h \tag{11}$$

V_x and V_z are components of reference velocity along the x and z axes, V is the reference velocity magnitude, μ is the gravitation parameter, and h is the angular momentum. To first order in e, the secular errors due to neglecting e are then given by Eqs. (1–4) with $k = 1.5\mu/ha$.

In summary, the circular orbit equations can be used to describe perturbed motion about a moderately elliptic reference orbit if the relative position vector is expressed in a local tangent coordinate system. The accuracy is probably more than adequate for many applications including manual rendezvous in earth orbit, up to an eccentricity of 0.05.

References

[1] Clohessy, W. H. and Wiltshire, R. S., "Terminal Guidance System for Satellite Rendezvous," *Journal of the Aerospace Sciences*, Vol. 27, No. 9, Sept. 1960, pp. 653–658, 674.

[2] Steffan, K. L., "Orbital Guidance," *Guidance of Aerospace Vehicles*, edited by C. T. Leondes, McGraw-Hill, New York, 1963, pp. 426–458.

[3] Schneider, A. M., Prussing, J. E., and Timin, M. E., "A Manual Method for Space Rendezvous Navigation and Guidance," *Journal of Spacecraft and Rockets*, Vol. 6, No. 9, Sept. 1969, pp. 998–1006.

[4] Stern, R. G., "Interplanetary Midcourse Guidance Analysis," Sc.D. thesis, 1963, Dept. of Aeronautics and Astronautics, Massachusetts Institute of Technology.

[5] Alspach, D. L., "Solutions to the Homogeneous Equation for Arbitrary Eccentricity," Subappendix 5 to Appendix XXI of Schneider, A. M., Prussing, J. E., and Timin, M. E., *Manual Techniques for Spacecraft Rendezvous and Reentry*, Rept. AFAL-TR-68-300, Nov. 2, 1968, Air Force Avionics Lab., Wright-Patterson Air Force Base, Ohio.

[6] Tschauner, J., "Elliptic Orbit Rendezvous," *AIAA Journal*, Vol. 5, No. 6, June 1967, pp 1110–1114.

[7] Schneider, A. M. and Koble, H. M., "Eccentricity Error of Dynamical Equations Linearized about a Circular Orbit," Rept. SDC-1-69, Aug. 18, 1969, Dept. of Aerospace and Mechanical Engineering Sciences, University of California at San Diego; also Revision A, May 1, 1970.

Random Vibration Response of Cantilever Plates Using the Finite Element Method

Alfred T. Jones* and Charles W. Beadle†
University of California, Davis, Calif.

Nomenclature

E	= Young's modulus, lbf/in.^{2}
f_n	= nth generalized force, lbf
$f(x,y,t)$	= driving force, lbf
$H(\omega)$	= frequency transfer function, g/lbf
m_n	= nth generalized mass, lbf-sec^2/in.
N	= total number of data points used in spectral analysis
PSD	= power spectral density
$S_a(\omega)$	= acceleration spectral density, g^2/cps
$S_f(\omega)$	= driving force spectral density, lbf^2/cps
T	= total time length of signal segment used in spectral analysis, sec
t	= time, sec
$\{w\}$	= $n \times 1$ column matrix representing discretized plate displacement
ζ_n	= nth modal damping ratio
ω_n	= nth natural frequency
ν	= Poisson's ratio
$\{\Phi_n\}$	= $n \times 1$ column matrix representing nth eigenvector
Ψ_n	= nth phase angle
τ	= sampling period, sec

Introduction

ANALYSIS of structures subjected to random excitation has become an important problem. With deterministic excitation, an undamped model was usually sufficient to describe motion, but random signals have energy present in most

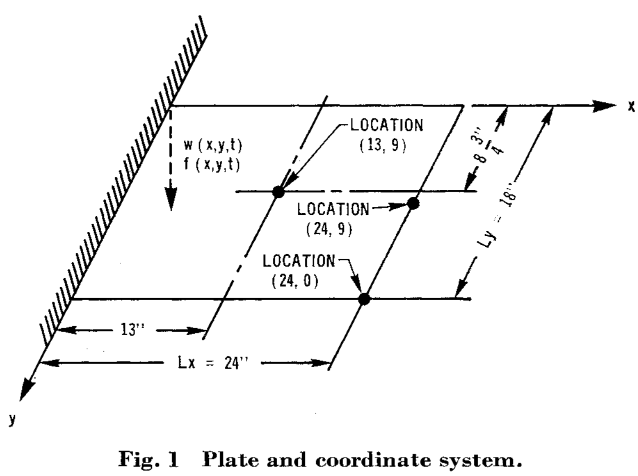

Fig. 1 Plate and coordinate system.

Received December 11, 1969; revision received May 27, 1970.

* Presently Staff member, Sandia Laboratories, Livermore, Calif.

† Associate Professor of Mechanical Engineering.

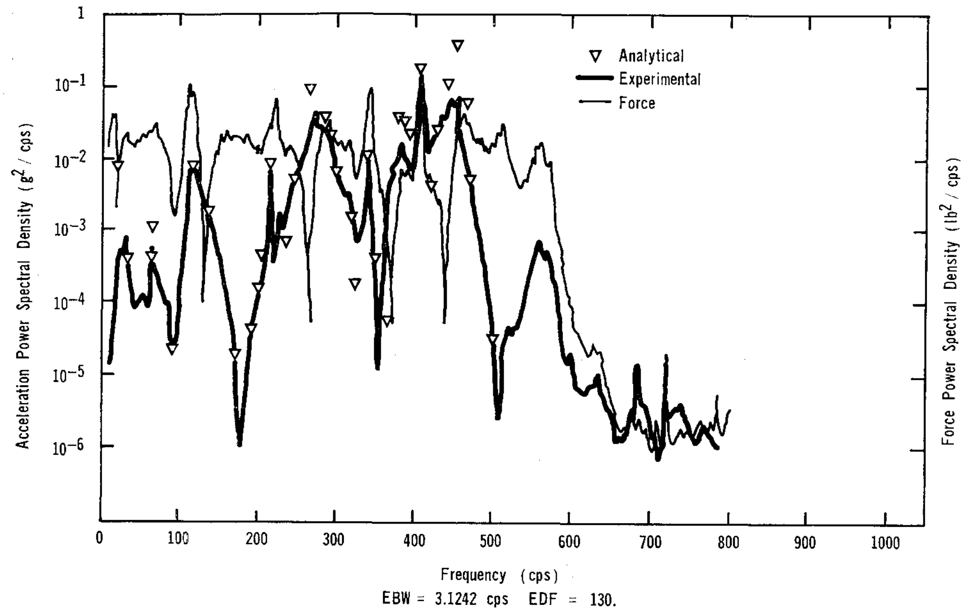

Fig. 2 Input and output power spectral densities at location (24,0).

parts of the spectrum. This results in instabilities in the analytical model unless damping is added.

The cantilever plate problem has no useful closed form solution for general static or dynamic loads. This study used the finite element procedure to analyze the plate which is described in Fig. 1. The model was then used to predict the response PSD, using modal damping. Experiments were performed to verify the theoretical work.

Use of the finite element procedure for plate vibration is discussed by Anderson, et al.[1] The subject of random vibration of continuous structures is covered in papers by Stanisic,[6] Thompson,[7] and Eringen.[4] Newsom, Fuller, and Sherrer[5] report on the finite element analysis of beams subject to random excitation. Trubert[8] presents experimental PSD investigation of structures using experimentally derived transfer functions.

Details of the finite element procedure

The plate dynamics were analyzed by modal expansion. Eigenvectors and natural frequencies were calculated using the finite element procedure. The noncompatible rectangular element described by Melosh[9] was used. Corner rotation variables were eliminated from the stiffness matrix by partitioning as recommended by Anderson et al.[1] The mass matrix was derived by distributing one quarter of the mass of the element to each corner point. Experimental natural frequencies and mode shapes were well fit by the procedure using 100 displacement coordinates.

Experimental sinusoidal and random excitation tests

To extend undamped analysis to the analysis of random excitation, it was necessary to determine damping factors, so a swept sinusoidal excitation test was performed on a model plate. The plate was made of 6016-T6 aluminum with dimensions: span, 24.0 in.; chord, 18.0 in.; and thickness, 0.360 in. and material properties $E = 10.1 \times 10^6$ lbf/in.,^{2} $\nu = 0.33$, $m = 0.098$ lbf/in^3. A Spectral Dynamics 1002B mechanical impedance system was used to perform the test with the driving force at (13,9) and monitoring accelerations at (24,0) and (24,9).

Modal damping was used to describe the plate damping. The response for the plate to a force of $f \sin(\omega t)$, can be written

$$w_i = \left[\left(\sum_{n=1}^{N} a_{in} \cos\psi_n\right)^2 + \left(\sum_{n=1}^{N} a_{in} \sin\psi_n\right)^2\right]^{1/2} \times \sin(\omega t - \Psi) \quad (1)$$

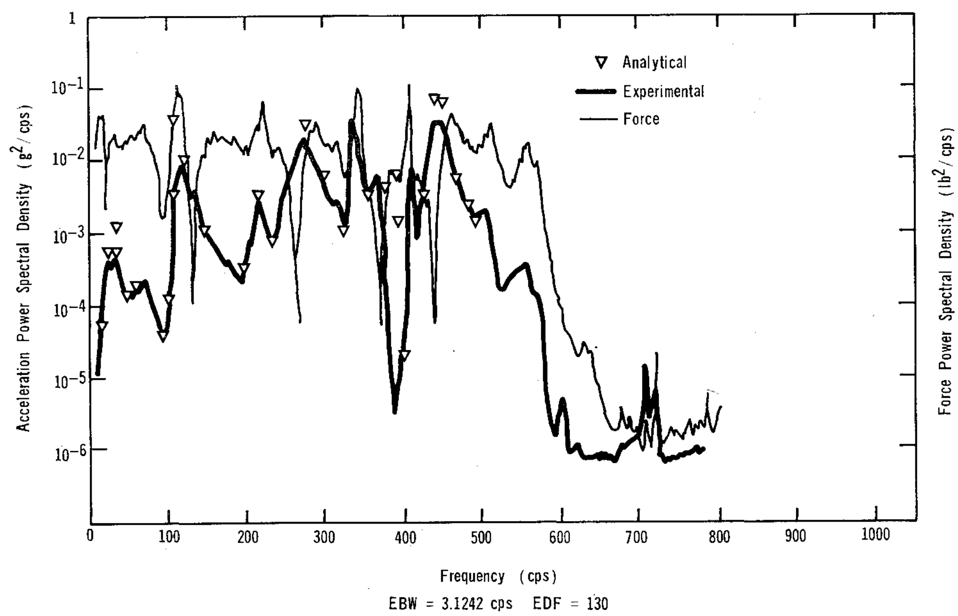

Fig. 3 Input and output power spectral densities at location (24,9).

where

$$\Psi = \frac{\sum_{n=1}^{N} \sin\psi_n}{\sum_{n=1}^{N} \cos\psi_n}$$

$$a_{in} = \frac{\Phi_{in} f_n}{m_n[(\omega_n^2 - \omega^2)^2 + (2\omega_n\omega\zeta_n)^2]^{1/2}}$$

$$\psi_n = \tan^{-1} \frac{2\omega_n\,\omega\zeta_n}{\omega_n^2 - \omega^2} \qquad (2)$$

where Φ_{in} and w_i mean the ith entry of the nth modal vector and displacement vector, respectively. Each ζ_n can be determined from the frequency response curves, noting that the maximum acceleration (for light damping) at the jth natural frequency is

$$\{\ddot{w}\}_{\max} = \{\Phi\}_j f_j / 2m_j\zeta_j \qquad (3)$$

The quantities m_j, f_j, and $\{\Phi\}_j$ were determined from the finite element computer program, and ζ_j was then calculated from Eq. (3), using $\{\ddot{w}\}_{\max}$. The results, comparing frequency transfer functions, show good agreement with the experiment, using the first 10 modes.

The plate was then driven by a random signal at point (13,9). Accelerations were monitored at locations (24,0) and (24,9). The system used consisted of a Calidyne 150 pound shaker, a General Radio Noise generator, and an MB Electronics T388 Automatic Equalization System. The input was a "flat" band limited signal of level 0.00125 lb^2/cps and 500 cps bandwidth presented in Figs. 2 and 3. It was impossible to equalize the input spectrum so that the spectrum at the shaker table was flat, because the equalization filters had a gain of only ±40 db relative to each other. Resonances with gains of 40 db occurred, so the signal occasionally would exceed the limits of the filter amplifiers. This made the input spectrum rough. Thirty seconds of data from the shaker table and each of the two accelerometers were recorded on analog tape and then digitized. The sampling rate was 5 kc and fixed the Nyquist frequency at 2.5 kc.

The random data were analyzed for their spectral density according to the modified periodogram approach proposed by Welch.[3] The data window used in this analysis was the function

$$D(t) = 1 - |t|/T \quad |t| \leq T$$
$$= 0 \quad |t| > T \qquad (4)$$

which is the Parzen spectral window. The equivalent window bandwidth (EBW) is $\Delta\omega = 16.1/\tau(L + 1)$, where the total record is broken up into L segments which overlap each other halfway. The modified periodogram was calculated for each segment sequentially and the L modified periodograms were averaged. The variance of the PSD can be given by equivalent degrees of freedom (EDF) which is $EDF = 3.6\,N/(L-1)$

For the tests conducted, $\Delta f = \Delta\omega/2\pi = 3.1$ cps and EDF = 130. The bandwidth is narrow enough to resolve most of the peaks, and the variance is low.

Results and comparisons to theory

It is shown in Thompson[7] and elsewhere that

$$S_a(\omega) = |H(\omega)|^2\, S_f(\omega) \qquad (5)$$

Figures 2 and 3 present this relationship. Analytically derived $S_a(\omega)$ from Eq. (1) were used to construct the triangular points on these figures, using Eq. (5) and the input shown in Figs. 2 and 3 as thin lines. The heavy solid lines represent completely experimental $S_a(\omega)$ data. The agreement appears adequate.

There are points which do not agree well with the experiment at the resonant peaks. There is an overshoot of the analytically derived spectra at these frequencies, which is quite severe. This is mainly caused by "leakage." From the experimental input curve, it can be seen that neighboring each peak is a deep valley. As the Parzen window is convolved onto the true experimental spectrum, the presence of the valleys is felt at adjacent peaks, and vice versa. Even a 3.1 cps bandwidth window cannot compensate for the total test dynamics. The spectrum calculated by Eq. (5), has, in effect, skipped the final windowing that was unavoidably done to the experimental spectrum. When the force spectrum in Fig. 2 or 3 is physically passed through the plate, it has the plate dynamics superimposed on it. These dynamics tend to "roughen" the experimental spectrum, which is then unavoidably windowed in the process of deriving Figs. 2 and 3.

Further proof of this hypothesis is provided by Fig. 3 which is the acceleration PSD at (24,9). The transfer function for this plot is smoother than the others, and consequently the data agree better. The analytical curve in Fig. 3 still is somewhat inaccurate at certain resonances, however. These are instances where the analytic transfer functions are inaccurate.

It is felt that the only effective cure for this problem is to prewhiten the data by applying a series of prewhitening filters to flatten the spectrum. However, raw data must be analyzed, then prewhitened on the basis of the raw data analysis, then the PSD computed again. The final PSD can be postdarkened to resemble the true spectrum.

References

[1] Anderson, R. G. et al., "Vibration and Stability of Plates Using the Finite Element Method," *International Journal of Solids and Structures*, Vol. 4, No. 10, pp. 1031–1055.

[2] Claassen, R. W. and Thorn, C. J., "Vibrations of a Rectangular Cantilever Plate," PMR TR 61-1, Aug. 1962, Pacific Missile Range, Point Mugu, Calif.

[3] Welch, P. W. et al., "The Fast Fourier Transform and Its Applications," Research Paper R. C. 1743, 1967, IBM, Yorktown Heights, N. Y.

[4] Eringen, A. C., "Response of Beams and Plates to Random Loads," *Transactions of ASME*, Series E, Vol. 24, No. 1, 1957, pp. 46–52.

[5] Newsom, C. D., Fuller, J. R., and Sherrer, R. E., "A Finite Element Approach for the Analysis of Randomly Excited, Complex, Elastic Structures," *Joint AIAA-ASME Conference on Structures, Structural Dynamics and Materials*, 1967, pp. 125–32.

[6] Stanisic, M. M., "Response of Plates to Random Load," *Journal of Acoustical Society of America*, Vol. 43, No. 6, 1968, pp. 1351–7.

[7] Thompson, W. T., "Continuous Structures Excited by Correlated Random Forces," *International Journal of Mechanical Sciences*, Vol. 4, March–April 1962, pp. 109–14.

[8] Trubert, M. R. P., "Response of Structures to Statistically Correlated Multiple Random Excitations," *Journal of the Acoustical Society of America*, Vol. 35, No. 7, 1963, pp. 1009–22.

[9] Zienkiewicz, O. C. and Cheung, Y. K., *The Finite Element Method*, McGraw-Hill, London, 1967, p. 92.

Fog Dispersal By High-Power Lasers

GEORGE W. SUTTON*
Avco Everett Research Laboratory, Everett, Mass.

Nomenclature

a = sound speed $(\gamma kT/M)^{1/2}$
A = constant, Eq. (22)
c_p = specific heat at constant pressure

Received June 9, 1970; revision received July 22, 1970. This work was supported by the AVCO Independent Research and Development Program.

* Scientist. Fellow AIAA.